Lithos 190–191 (2014) 430–439

Contents lists available at ScienceDirect

Lithos

journal homepage: www.elsevier.com/locate/lithos

The Permian–Triassic granitoids in Bayan Obo, North China Craton: A geochemical and geochronological study

Ming-Xing Ling [a,*], Hong Zhang [b], He Li [c], Yu-Long Liu [c], Jian Liu [d], Lin-Qing Li [e], Cong-Ying Li [c], Xiao-Yong Yang [f], Weidong Sun [c,*]

[a] State Key Laboratory of Isotope Geochemistry, Guangzhou Institute of Geochemistry, Chinese Academy of Sciences, Guangzhou 510640, China
[b] State Key Laboratory of Continental Dynamics, Department of Geology, Northwest University, Xi'an 710069, China
[c] CAS Key Laboratory of Mineralogy and Metallogeny, Guangzhou Institute of Geochemistry, Chinese Academy of Sciences, Guangzhou 510640, China
[d] Zhejiang Institute of Geological Survey, Hangzhou 311203, China
[e] Hebei Institute of Regional Geology and Mineral Resources Survey, Langfang 065000, China
[f] CAS Key Laboratory of Crust–Mantle Materials and Environments, School of Earth and Space Sciences, University of Science and Technology of China, Hefei 230026, China

ARTICLE INFO

Article history:
Received 12 October 2013
Accepted 4 January 2014
Available online 13 January 2014

Keywords:
North China Craton (NCC)
Bayan Obo
Granitoids
Rare earth element deposit
Zircon U–Pb dating
Permian–Triassic

ABSTRACT

Granitoids near the Bayan Obo giant rare earth element (REE) deposit at the north margin of the North China Craton (NCC), the world's largest light REE (LREE) deposit, have been taken by some authors as the key factors that controlled the mineralization. In contrast, others proposed that the REE deposit has been partially destructed by these granitoids. Here we report systematic studies on geochronology and geochemical characteristics of granitoids of different distances from the orebodies, to investigate the genesis and their relationship to the giant Bayan Obo deposit. Granitoids studied here, including granites and quartz monzonites, are peraluminous with A/CNK = 0.99–1.11, LREE enriched and heavy REE (HREE) depleted, with variable REE concentrations (total REE = 54–330 ppm) and large negative Eu anomaly (δEu = 0.19–0.70). The REE patterns are distinct from those of ore-bearing dolomites. Some samples have slightly higher LREE concentrations, which may have been contaminated by the orebodies during intrusion. Trace elements of the granitoids are characterized by positive Pb anomaly, strong negative Ti anomaly and Nb, Ta and Sr anomalies. The granites exhibit negative Ba anomaly. The granitoids plot within the post-collision granite field in the Pearce diagram, which is consistent with the tectonic regime. The quartz monzonites and one granite have A-type granite characteristics and belong to the A_2 subgroup. Zircons in these granitoids have high Th/U values, which are typical for magmatic zircons. High precision U–Pb dating for these zircons by secondary ion mass spectrometry (SIMS) and laser ablation inductively coupled plasma mass spectrometry (LA–ICP-MS) yields Permian–Triassic $^{206}Pb/^{238}U$ ages ranging from 243.2 to 293.8 Ma. The formation of the granitoids is >55 Ma later than the latest ore forming age. The zircons have low La concentrations (0.02–12 ppm), high $(Sm/La)_N$ (0.8–685) and Ce/Ce^* (1.4–80). The Ti-in-zircon temperature of the granitoids ranges from 590 to 770 °C. All these evidences suggest that the granitoids have no contribution to the formation of the Bayan Obo deposit. Granitoids that are close to the orebodies had limited interaction with it and gained some LREE-enriched characteristics during magmatisms. Nevertheless, their effects to the orebodies are subtle. All the granitoids formed in a post-collisional tectonic regime at convergent margins, which is consistent with plate subduction during the closure of the Palaeo-Asian Ocean, which started in the Neoproterozoic and lasted until the Carboniferous/Permian.

1. Introduction

Bayan Obo, located at the northern margin of the North China Craton (NCC) (Fig. 1), is the largest light rare earth element (REE) deposit in the world, the largest niobium (Nb) and thorium (Th) deposit, and a major iron (Fe) deposit in China (Chao et al., 1992; Kynicky et al., 2012; Lai and Yang, 2013; Ling et al., 2013; Y.L. Liu et al., 2008; Tu, 1998; Yang and Le Bas, 2004; Yang et al., 2009; Yuan et al., 1992). Granitoids are widespread near the Bayan Obo deposit (Fig. 1), which have been studied by several groups (Chao et al., 1997; Fan et al., 2009; Ling et al., 2013; Wang, 1980; Wang et al., 1973, 1994; Yang et al., 2000; Yuan et al., 1992). These granitoids were taken by some authors as the key factors that controlled the mineralization (IGCAS, 1988; Wang et al., 1973), while others proposed that the REE deposit has been partially transformed and further metasomatized by the granitoid intrusion (Yuan et al., 1992), but little REE ore-forming material was brought into the orebodies (Yuan et al., 1992). Recent studies favor that there is no connection between the granitoids and the formation of the REE deposit (Fan et al., 2009; Ling et al., 2013; Yang et al., 2000). Nevertheless,

* Corresponding authors.
E-mail addresses: mxling@gig.ac.cn (M.-X. Ling), weidongsun@gig.ac.cn (W. Sun).

0024-4937/$ – see front matter © 2014 Elsevier B.V. All rights reserved.
http://dx.doi.org/10.1016/j.lithos.2014.01.002

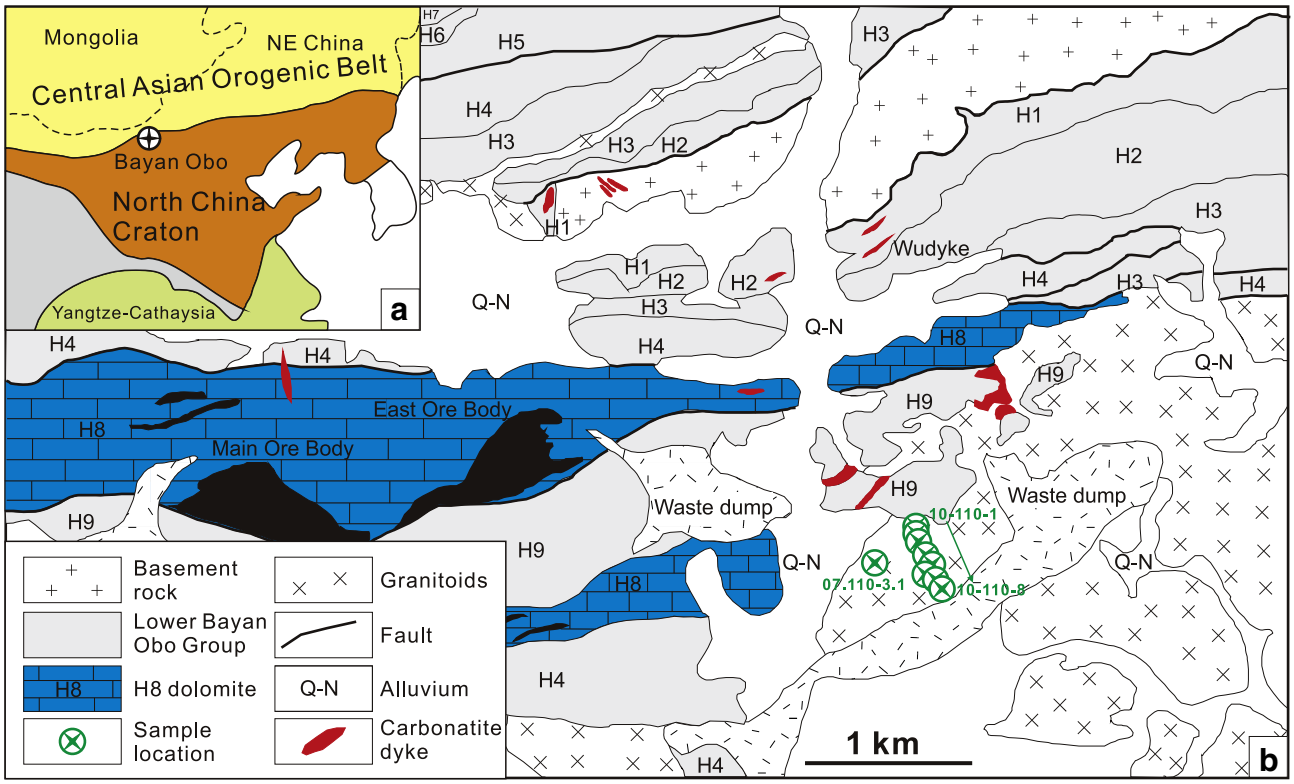

Fig. 1. Geological setting in Bayan Obo, North China Craton. (a) Simplified map showing the location of Bayan Obo, the North China Craton, and the Central Asian Orogenic Belt, modified after Jahn et al. (2000) (b) Sketch geological map of Bayan Obo, showing the Triassic–Permian granitoids and the sample locations, modified after Y.L. Liu et al. (2008) and Ling et al. (2013).

granitoids contacting with the orebodies do have higher REE content than others (Wang, 1980). Given that most previous dating of the granitoids gives Permian ages, e.g., K–Ar age 246–270 Ma (IGCAS, 1988), Rb–Sr isochron age 264 ± 91 Ma or 249 ± 35 Ma (Zhang et al., 2003), Rb–Sr isochron age 255.2 ± 8.2 Ma (Wang et al., 1994, and references therein), 263–273 Ma by LA–ICP-MS zircon U–Pb dating (Fan et al., 2009), and 267.4 ± 2.2 Ma by SIMS zircon U–Pb dating (Ling et al., 2013), it has been argued that the granitoids made no contribution to the mineralization (Ling et al., 2013). Nevertheless, there are large volumes of granitoid intrusions near the Bayan Obo region. Only a few have been dated, and there is no systematic geochemical data yet reported. In addition, many of the previously reported ages were not done using suitable methods, and the ages varied dramatically with large uncertainties. Moreover, these granitoids may have negative effects in the form of remobilization and grade reduction on the Bayan Obo deposit, which have not been previously studied.

To test these possibilities, we sampled a granitoid profile of ~800 m from the southeast boundary of the Bayan Obo deposit outward, and carried out a detailed geochemical study, aiming at better constraints on the genesis of these granitoids and their relation to the Bayan Obo deposit.

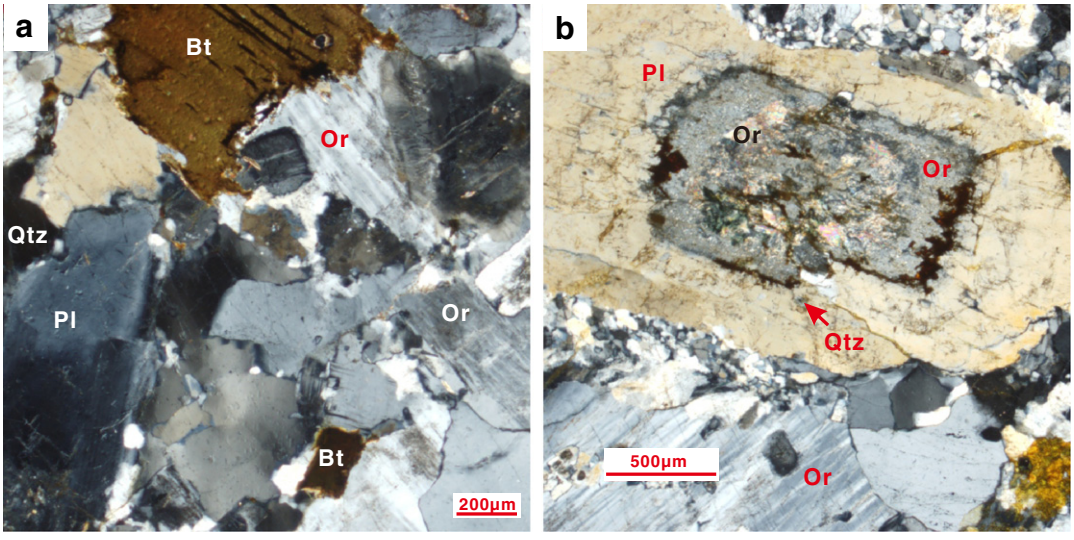

Fig. 2. Cross-polarized microscopic photos of the granitoids. Qtz = quartz, Pl = plagioclase, Or = orthoclase, Bt = biotite.

Table 1
Major and trace element compositions of the granitoids from Bayan Obo (major elements: %; trace elements: ppm).

Sample	10-110-1	10-110-2	10-110-3	10-110-4	10-110-5	10-110-6	10-110-7	10-110-8	07.110-3.1
Rock type	Quartz monzonite	Granite	Granite	Granite	Quartz monzonite	Quartz monzonite	Quartz monzonite	Granite	Granite
SiO_2	69.70	76.32	72.78	76.50	66.48	65.75	68.65	73.83	73.02
TiO_2	0.34	0.04	0.17	0.02	0.36	0.38	0.28	0.15	0.24
Al_2O_3	15.18	12.93	13.76	13.21	16.21	16.67	15.68	13.40	13.82
$Fe_2O_3^T$	2.72	0.70	1.98	0.68	3.35	3.64	2.92	1.73	1.92
MnO	0.11	0.11	0.07	0.06	0.09	0.10	0.08	0.04	0.04
MgO	0.55	0.09	0.30	0.09	0.61	0.62	0.47	0.27	0.48
CaO	1.63	0.46	0.94	0.57	2.01	2.12	1.44	0.78	1.15
Na_2O	4.23	3.84	3.46	4.10	4.08	3.93	3.91	3.52	3.57
K_2O	5.03	4.79	5.05	4.48	5.01	5.15	5.05	4.48	4.76
P_2O_5	0.11	0.01	0.08	0.01	0.10	0.15	0.08	0.08	0.06
LOI	0.35	0.39	0.40	0.25	0.46	0.52	0.52	0.59	0.35
Total	100.15	99.69	99.07	100.00	98.99	99.28	99.27	98.94	99.42
A/CNK	0.99	1.05	1.07	1.05	1.03	1.05	1.08	1.11	1.05
Cs	4.85	6.42	5.50	2.20	3.50	3.18	4.13	3.95	4.90
Rb	189	249	187	164	137	132	154	185	136
Ba	1275	91	692	181	1765	1855	1380	568	567
Th	21.2	33.0	22.1	28.9	16.1	16.9	17.7	30.7	11.9
U	3.49	2.36	2.62	1.30	2.33	1.57	2.09	5.78	2.53
Nb	24.4	18.1	13.5	18.1	16.8	15.6	16.4	17.6	12.2
Ta	2.10	4.10	1.20	4.10	0.80	0.70	0.90	1.40	0.77
La	42.7	10.0	30.4	5.40	83.0	65.8	47.8	30.7	25.7
Ce	81.6	22.8	52.7	15.1	150	137	140	57.8	46.7
Pb	29.0	41.0	29.0	16.0	24.0	20.0	25.0	25.0	20.0
Pr	9.73	3.06	6.21	1.94	15.7	13.3	9.31	6.34	5.04
Sr	325	34.4	142	79.5	352	340	247	120	130
Nd	35.7	11.9	22.0	8.20	51.6	46.4	30.8	20.9	19.5
Sm	7.14	3.34	3.97	2.76	7.81	7.62	5.62	3.67	3.89
Zr	305	67	163	58	348	391	307	157	183
Hf	8.80	4.70	5.00	4.50	8.50	9.60	8.00	4.90	4.81
Eu	1.27	0.21	0.79	0.28	1.77	1.71	1.29	0.62	0.69
Ti	1902	224	951	112	2014	2126	1567	839	1220
Gd	6.71	3.36	3.82	3.11	7.71	7.32	5.73	3.54	3.43
Tb	1.06	0.63	0.57	0.69	0.99	0.96	0.83	0.50	0.50
Dy	6.05	4.17	3.14	4.70	4.88	4.96	4.44	2.74	3.03
Y	38.1	28.6	17.7	31.2	25.1	24.6	24.2	16.2	16.6
Ho	1.27	0.91	0.63	1.09	0.95	0.93	0.91	0.57	0.64
Er	4.03	3.15	2.00	3.79	2.82	2.80	2.69	1.88	1.74
Tm	0.62	0.53	0.31	0.66	0.37	0.34	0.36	0.29	0.27
Yb	4.38	4.19	2.16	5.20	2.48	2.46	2.54	2.17	1.85
Lu	0.69	0.67	0.35	0.77	0.38	0.38	0.40	0.35	0.29
LREE/HREE	10.2	3.84	13.1	2.18	24.7	21.7	19.8	14.5	12.6
δEu	0.56	0.19	0.62	0.29	0.70	0.70	0.69	0.53	0.58
Ce/Ce*	0.94	1.00	0.89	1.14	0.95	1.07	1.53	0.96	0.94

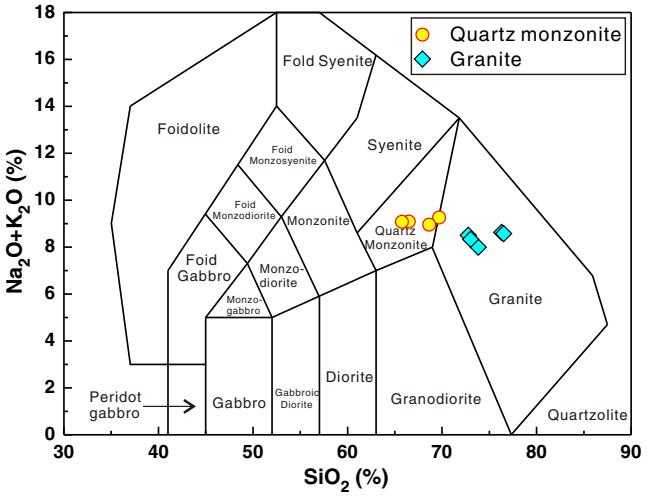

Fig. 3. Total alkalis versus SiO_2 (TAS) diagram. The samples fall in the quartz monzonite and granite fields. The yellow filled circles and blue filled diamonds represent quartz monzonite and granite, respectively.

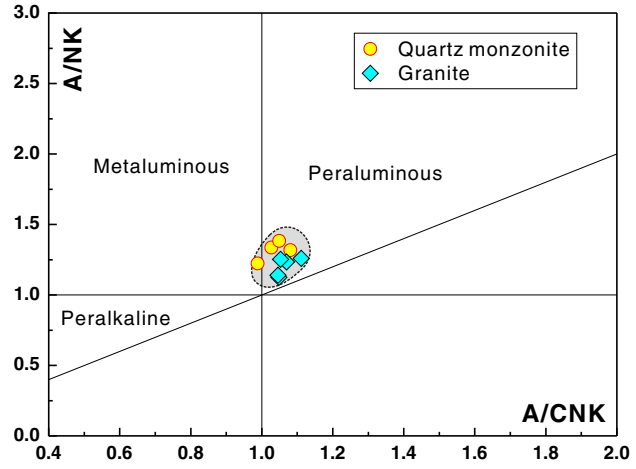

Fig. 4. A/NK versus A/CNK diagram (Shand, 1943). A/NK = $Al_2O_3/(Na_2O + K_2O)$ (molar ratio), A/CNK = $Al_2O_3/(CaO + Na_2O + K_2O)$ (molar ratio). The samples mainly fall in the peraluminous field.

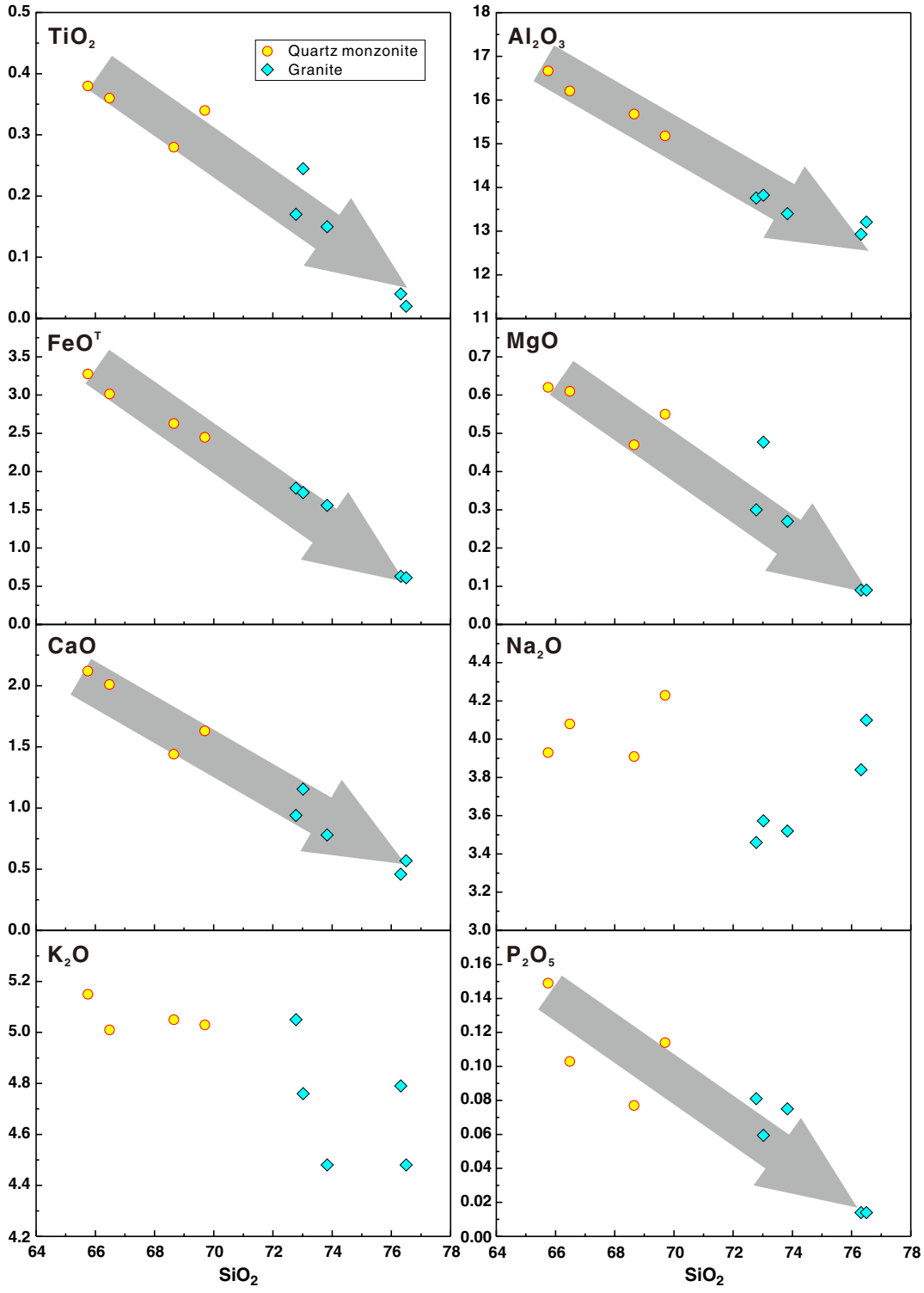

Fig. 5. Harker diagrams showing the major element variations of the granitoids in Bayan Obo. SiO_2 has clear negative correlation with Al_2O_3, FeO^T, TiO_2, MgO, CaO and P_2O_5, but no correlation with Na_2O and K_2O.

2. Geological background and samples

The Bayan Obo district, Inner Mongolia Autonomous Region, is located at the northern margin of the North China Craton (NCC), neighboring the south edge of the Central Asian Orogenic Belt (Ling et al., 2013; Yang et al., 2009) (Fig. 1). The giant Bayan Obo REE–Nb–Fe deposit is hosted in Palaeo- to Mesoproterozoic sediments of the Bayan Obo Group which consists of low-grade metamorphic sandstones, siltstones, limestones and dolomites and has been classified into two series, a lower regressive series (members H1–H10) and an upper transgressive series (H11–H20) (IGCAS, 1988). The REE deposit is hosted in the H8 dolomite (IGCAS, 1988; Lai et al., 2012; Ling et al., 2013; Y.L. Liu et al., 2008; Yang et al., 2009) (Fig. 1). The Bayan Obo Group was deposited upon an Archean basement of migmatites of the Wutai Group (Drew et al., 1990). Later studies showed that the basement in the Bayan Obo region is Early Proterozoic (Y.L. Liu et al., 2008). Large volumes of Palaeozoic

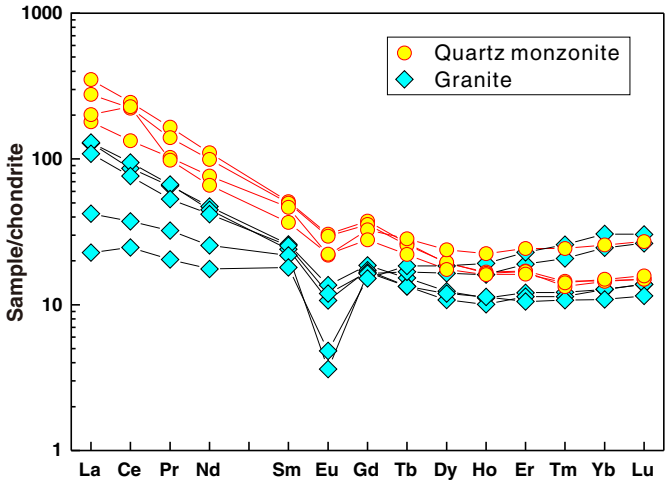

Fig. 6. Chondrite normalized REE patterns of the granitoids. Chondrite data are from Sun and McDonough (1989).

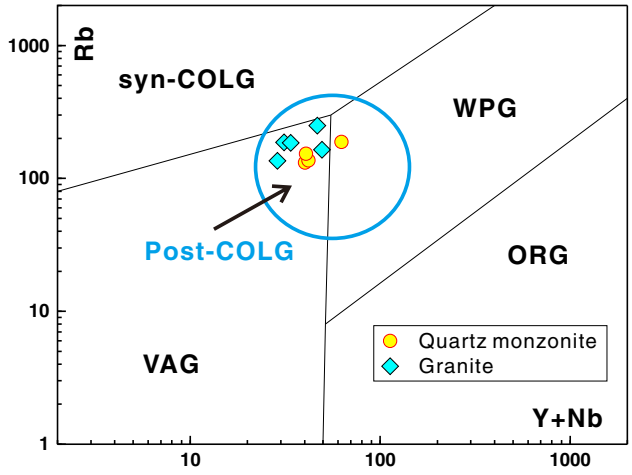

Fig. 8. Rb versus Y + Nb tectonic classification of the granitoids. The samples fall in the post-collision granite field. Syn-COLG = syn-collision granites, WPG = within plate granites, VAG = volcanic arc granites, ORG = ocean ridge granites, Post-COLG = post-collision granites.

granitoids intruded these rocks (Drew et al., 1990; Fan et al., 2009; IGCAS, 1988; Yang et al., 2000), and mainly outcropped south and east of the Bayan Obo ore deposit (Fig. 1). Four quartz monzonite and 5 granite granitoids were studied in this contribution. The granitoids are mainly composed of quartz (25–30 vol.%), plagioclase (20–25 vol.%), orthoclase (35–45 vol.%) and biotite (6–8 vol.%) (Fig. 2), with accessory minerals of magnetite, ilmenite, monazite, apatite and zircon.

3. Analytical methods

Fresh rocks were first ground to less than 200 mesh for major and trace element analysis. Sample rock powder was fluxed with lithium borate (sample/flux ratios 1:8) to make homogeneous glass disks for X-ray fluorescence (XRF) analysis, at 1150–1200 °C using a V8C automatic fusion machine produced by the Analymate Company in China. Analyses of major and trace elements were done at the State Key Laboratory of Isotope Geochemistry, Guangzhou Institute of Geochemistry, Chinese Academy of Sciences. Major elements were determined by Rigaku 100e XRF with analytical precision better than 1% (Ma et al., 2007). About 40 mg powders of each sample were accurately weighed and dissolved by a HF and HNO_3 mixture in screw-top Teflon beakers on a hot plate at the temperature of 150 °C in a clean laboratory. Sample solutions were dried and diluted to 3% HNO_3 with a factor of 1/2000. Rh was used as an internal standard for calibration. Trace elements were analyzed by Perkin-Elmer ELAN 6000 ICP-MS. Analytical precisions for trace elements are better than 5% (Liu et al., 1996).

Zircons were separated from samples by traditional heavy liquid and magnetic separation techniques, handpicked under a binocular microscope, mounted with epoxy resin and then polished down to near half sections to expose internal structures for SIMS and LA–ICP-MS analyses. Cathodoluminescence (CL) and optical microscopy images were used to inspect the zircon morphology and the clearest, least fractured rims of the zircon crystals were selected as suitable targets for laser ablation.

Zircon U–Pb dating of the sample 07.110-3.1 was performed at the State Key Lab of Lithospheric Evolution, Institute of Geology and Geophysics, Chinese Academy of Sciences, using a Cameca IMS 1280 SIMS following the procedures reported by Li et al. (2009). Temora was used as an external standard. The ellipsoidal spot is ~20–30 μm in size. The O_2^- primary ion beam was accelerated at −13 kV with an intensity of ~10 nA and positive secondary ions were extracted with a 10 kV potential. Zircon U–Pb dating and trace element analysis of other samples were conducted at the State Key Laboratory of Isotope Geochemistry, Guangzhou Institute of Geochemistry, by using a LA–ICP-MS system consisted of an Agilent 7500a ICP-MS coupled with a Resonetics RESOLution M-50 ArF-Excimer laser source (λ = 193 nm). The laser energy was 80 mJ, and the frequency was 6 Hz, with an ablation spot of 31 μm in diameter. Both a double-volume sampling cell and

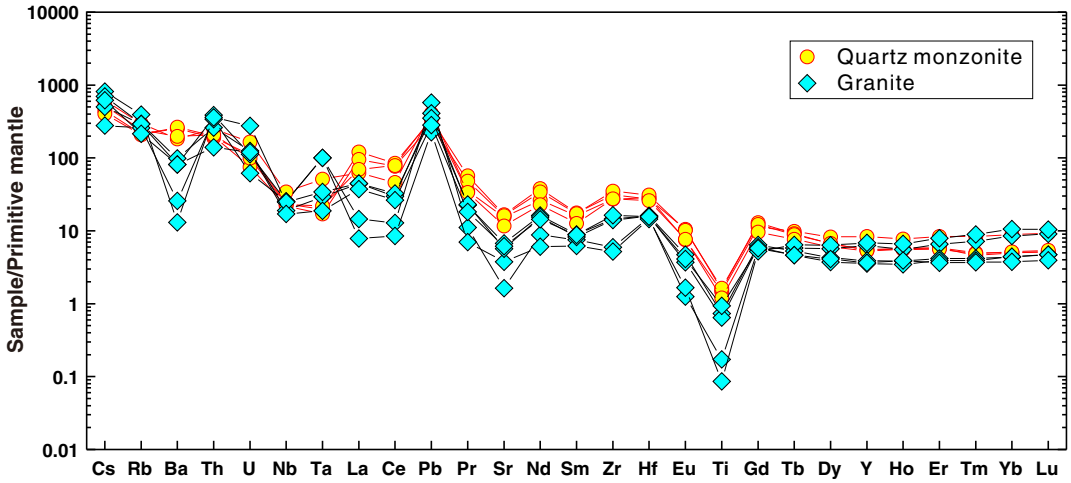

Fig. 7. Primitive mantle normalized trace element spider diagram of the granitoids. Primitive mantle data are from Sun and McDonough (1989).

a Squid smoothing device were used to improve the data quality. The ablated aerosol was carried to the ICP source with He gas. The detection limits of ICP-MS for trace elements are mostly better than 10 ppb, with uncertainties of 5–10%. Temora and NIST610 were used as external calibration standards for U–Pb dating and trace element analysis, respectively. ^{29}Si was taken as an internal standard for trace element (C.Y. Li et al., 2012; Liang et al., 2009; Tu et al., 2011). The data reduction of U–Pb dating and trace element analyses was performed by ICPMSDataCal (Y.S. Liu et al., 2008, 2010). Concordia diagrams and MSWD calculation were made using Isoplot 4.1 (Ludwig, 2012).

4. Results

4.1. Whole rock major and trace elements

Whole rock major and trace element results of the samples in this study are listed in Table 1. The samples have SiO_2 = 65.75–76.50 wt.% and total alkalis ($Na_2O + K_2O$ = 8.00–9.26 wt.%) and fall in the quartz monzonite and granite fields in the TAS diagram (Fig. 3). The granitoids are peraluminous with aluminum saturation indices A/CNK ($Al_2O_3/(CaO + Na_2O + K_2O)$) = 0.99–1.11 and A/NK ($Al_2O_3/(Na_2O + K_2O)$) = 1.12–1.38 (Fig. 4). In the Harker diagrams, SiO_2 has an obviously negative correlation with Al_2O_3, FeO^T, TiO_2, MgO, CaO and P_2O_5, but no correlation with Na_2O and K_2O (Fig. 5).

Chondrite-normalized REE patterns of these samples show LREE enriched and HREE depleted characteristics, and quartz monzonites have relatively higher LREE concentration than granite (Fig. 6). The granitoids exhibit a large negative anomaly (δEu) = 0.19–0.70 (Table 1), indicating removal of plagioclase by fractional crystallization during magma evolution, which is consistent with the negative Ba and Sr anomalies (Fig. 7). The Ce anomaly (Ce/Ce^*) is small, except sample 10-110-7 with positive Ce/Ce^* = 1.5 (Table 1). The samples have high and variable REE concentrations (total REE = 54–330 ppm). Some of the granitoids show variable LREE enrichment, which may have gained from the Bayan Obo REE orebodies during granitoid intrusion. Trace elements of the granitoids are characterized by positive Pb (16–41 ppm) anomaly and negative Nb (14–24 ppm), Ta (0.7–4.1 ppm), Ti (112–2126 ppm) and Sr (34–352 ppm) anomalies. The granites exhibit negative Ba anomaly (91–692 ppm) (Fig. 7, Table 1). All these granitoids plot within the post-collision granite field in the Rb vs. Y + Nb diagram (Fig. 8). Quartz monzonites and one granite have A-type granite characteristics (Fig. 9) and belong to A_2 subgroup (Fig. 10).

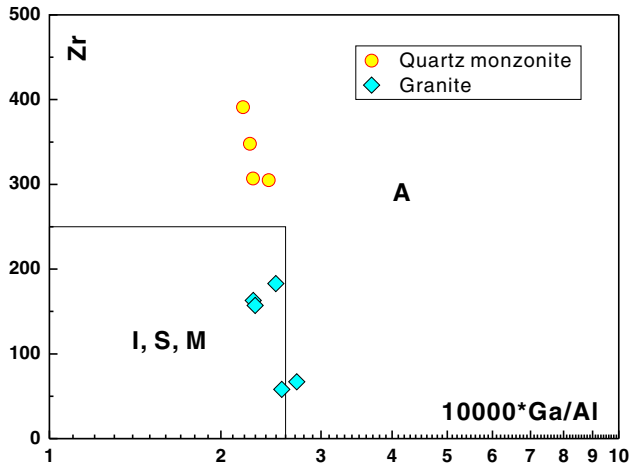

Fig. 9. Zr versus 10,000*Ga/Al discrimination diagram for granites (Pearce, 1996). Quartz monzonites and one granite have A-type granite characteristics.

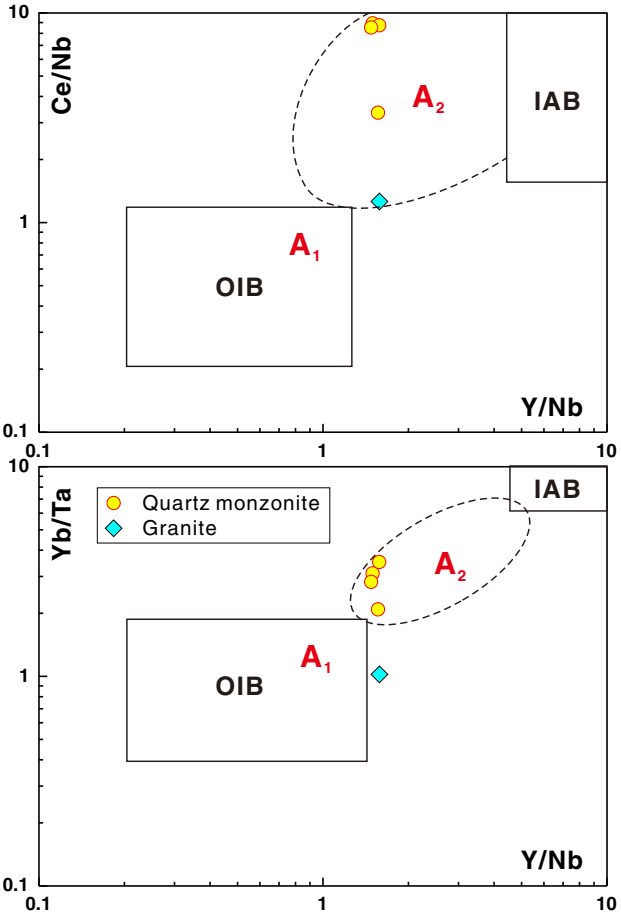

Fig. 10. A_1 and A_2 discrimination diagram for A-type granites.

4.2. Zircon U–Pb dating and trace element characteristics

Zircon U–Pb dating was conducted on all samples, SIMS dating for sample 07.110–3.1, and LA–ICP-MS analysis for the other samples. In total 116 zircon grains from 9 samples were analyzed. Zircon U–Pb dating results by LA–ICP-MS are listed in Supplementary Table S1.

CL images of the zircons display tight oscillatory zoning, which is typical of granitic zircons, consistent with high Th/U (0.4–1.0) (Fig. 11,

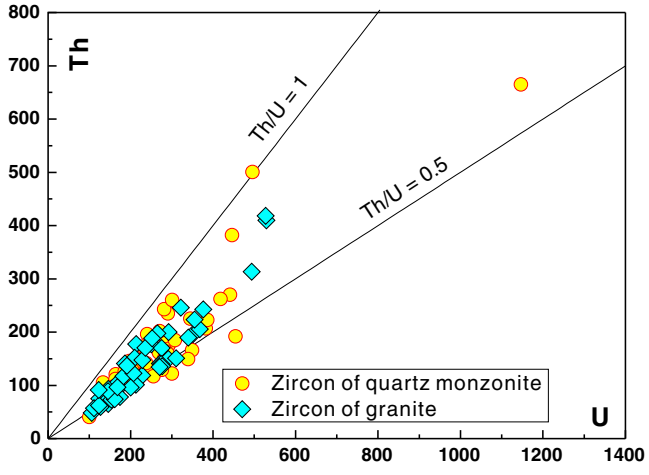

Fig. 11. Zircon Th–U diagram. Th/U ratios, mainly between 0.5 and 1.0 ratios of zircons indicate a magmatic origin. The yellow filled circles and blue filled diamonds represent zircons of quartz monzonite and granite, respectively.

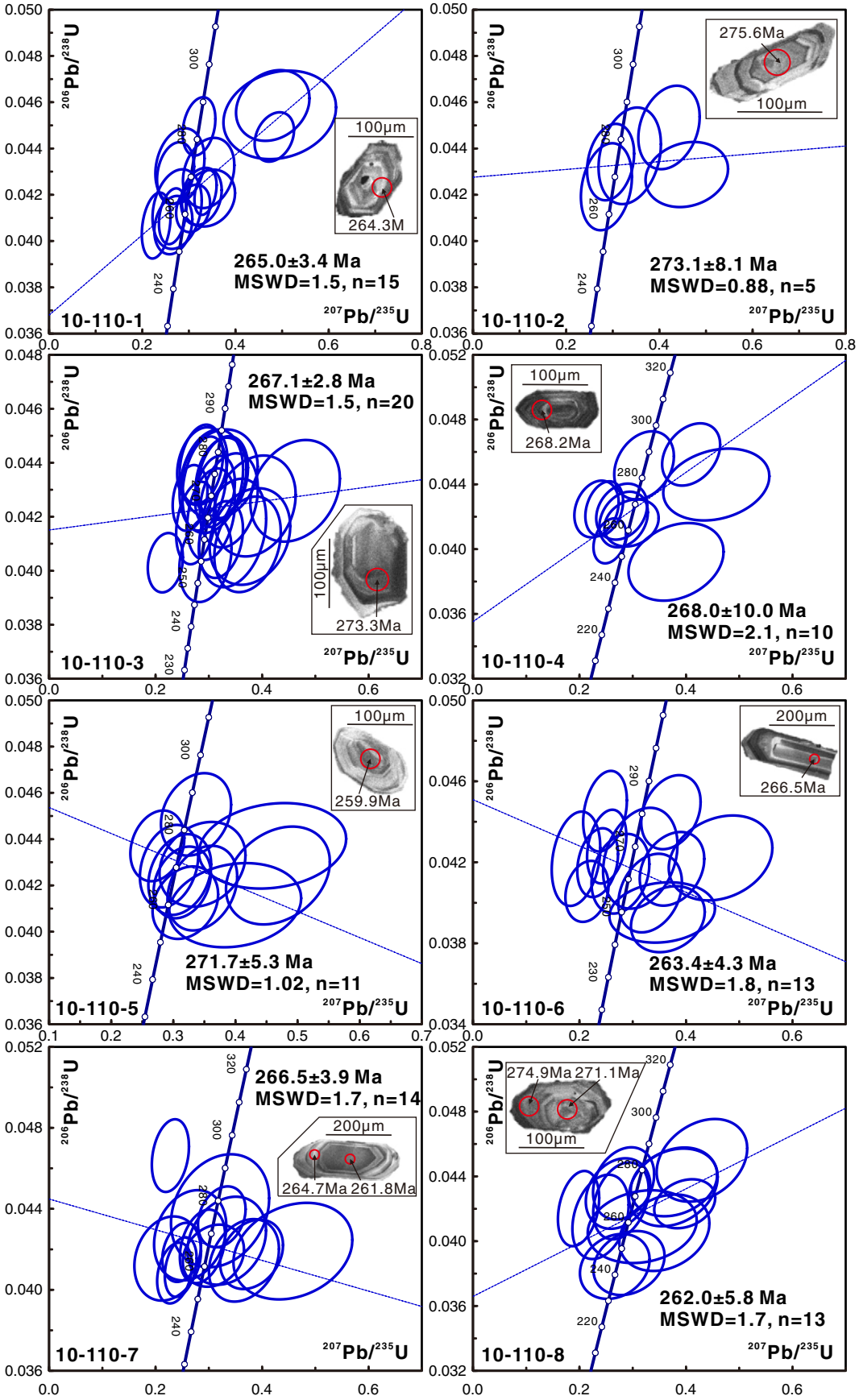

Fig. 12. Zircon U–Pb concordia diagrams of the granitoids. The intercept ages, MSWD of the concordia diagram, and the number of data points are presented, as well as CL image of typical zircons with laser spot sites and ages.

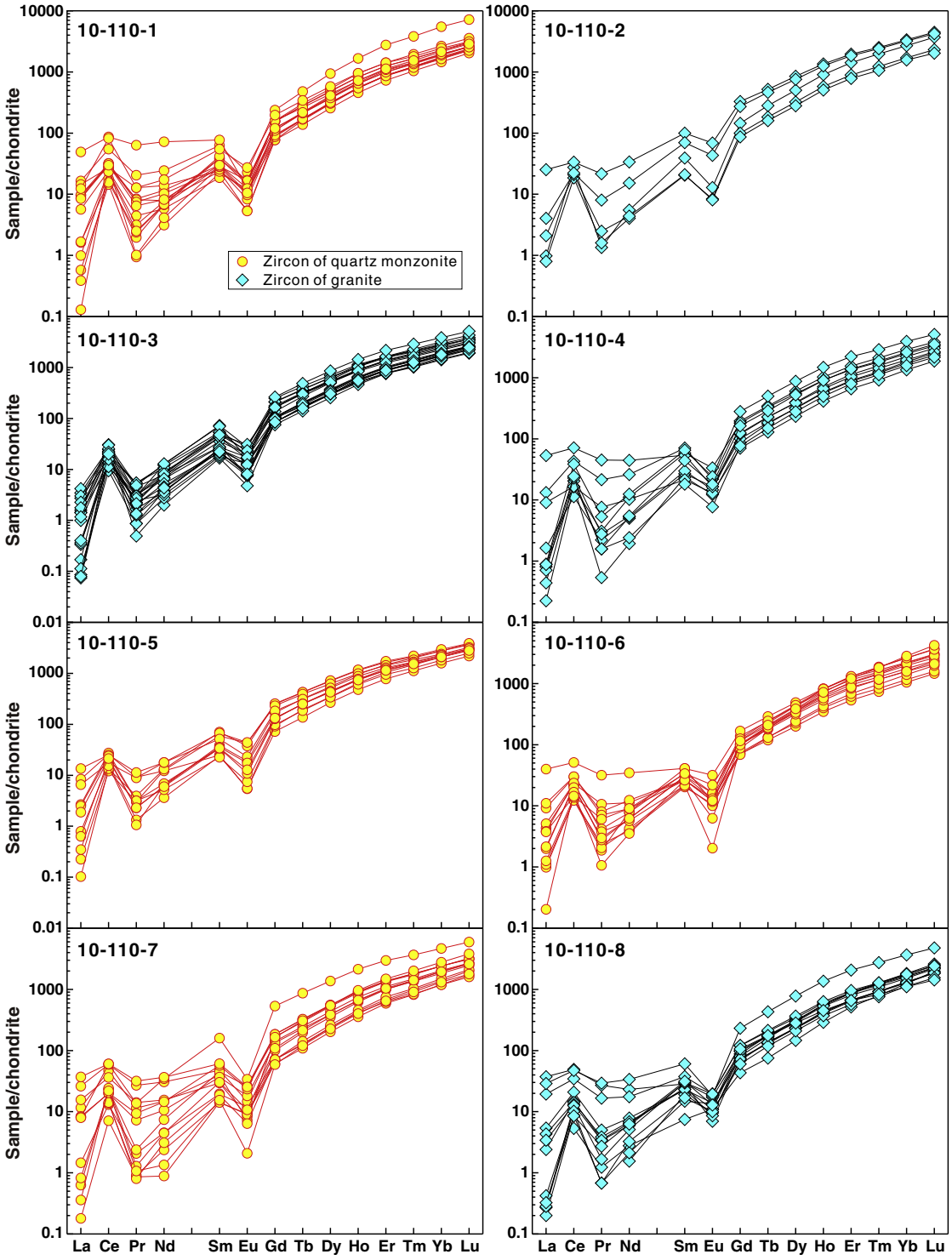

Fig. 13. REE pattern of zircons in the granitoids.
Chondrite data are from Sun and McDonough (1989).

Supplementary Table S1) (Hoskin and Schaltegger, 2003; Sun et al., 2002). SIMS zircon U–Pb dating for sample 07.110-3.1 yields $^{206}Pb/^{238}U$ age = 257.4–273.6 Ma (Ling et al., 2013). LA–ICP-MS analysis for zircons of other samples yields Permian–Triassic $^{206}Pb/^{238}U$ ages ranging from 243.2 to 293.8 Ma (Fig. 12, Supplementary Table S1), with a wider age range than SIMS results. The dating results show no clear age difference between granites and quartz monzonites. All these indicate that post-collisional granitoid activities in the Bayan Obo region lasted for ~50 Ma.

These zircons are LREE depleted and HREE enriched, with positive Ce anomaly and negative Eu anomaly. The zircons show largely scattered LREE concentrations, with much tighter HREE concentrations in the same sample (Fig. 13). The zircons have low La concentrations (0.02–12 ppm) (Supplementary Table S2), high $(Sm/La)_N$ (0.8–685) and Ce/Ce* (1.4–80) (Fig. 14).

The temperature of zircon formation ranges from 590 to 770 °C (Supplementary Table S2), based on Ti concentration in zircon (Watson et al., 2006). This is relatively lower but close to the

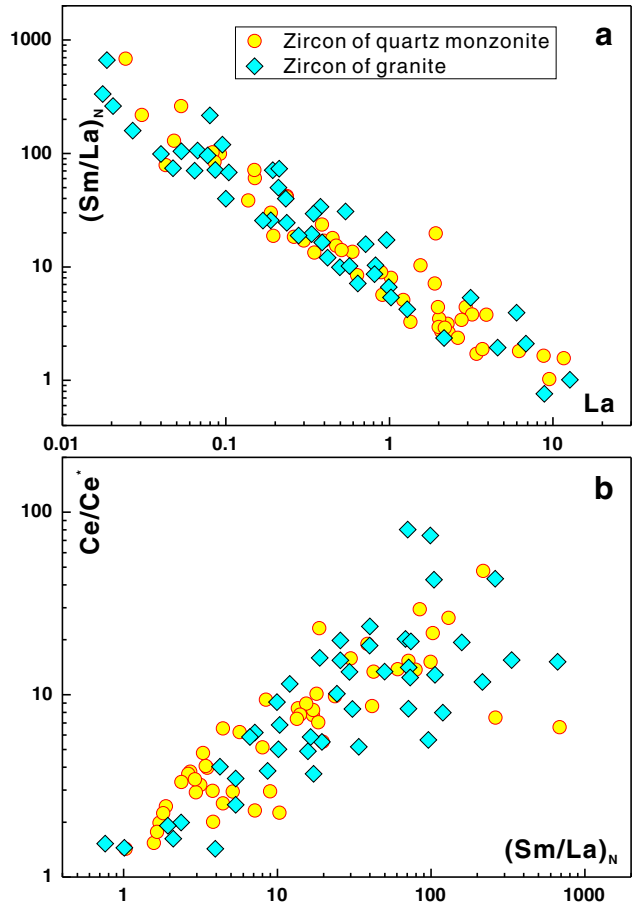

Fig. 14. $(Sm/La)_N$ versus La and Ce/Ce^* versus $(Sm/La)_N$ diagrams.

temperature of 640–870 °C of whole rock TiO_2–SiO_2 and P_2O_5–SiO_2 thermometers (Bea et al., 1992; Green and Pearson, 1986; Harrison and Watson, 1984).

5. Discussion

5.1. The geochemical characteristics of Permian–Triassic granitoids in Bayan Obo

The strong negative anomaly of Ti coupled with the less pronounced negative Nb and Ta anomalies (Fig. 7), implies the influence of ilmenite during fractional crystallization (H. Li et al., 2012). The zircon formation temperatures were a little low, ranging from 590 to 770 °C according to Ti-in-zircon thermometer (Supplementary Table S2) (Watson et al., 2006). The oxygen fugacity of these granitoids is low as indicated by Ce/Ce^* (Table 1), which is consistent with post-collisional settings.

As mentioned above, the granitoids plot within the post-collision granite field in the Rb vs. Y + Nb diagram (Fig. 8). Consistently, the A-type granites belong to the A_2 sub-group (Figs. 9 and 10). A-type granites (where A stands for alkaline, anorogenic and anhydrous, and aluminous) (Eby, 1992; H. Li et al., 2012) are characterized by hypersolvus to transsolvus to subsolvus alkali feldspar textures, iron-rich mafic mineralogy, bulk-rock compositions yielding ferroan alkali–calcic to alkaline affinities, and enrichment of incompatible trace elements, including LILE and HFSE (Bonin, 2007). A-type granite has been further divided into A_1 and A_2 chemical subgroups (Eby, 1992). A_1 granites have chemical characteristics similar to those observed for oceanic-island basalts. In contrast, A_2 granites are similar to rocks of continental crust or island-arc origins in chemical characteristics, and are attributed to continental crust at convergent margins (Eby, 1992). The A-type granites in this study are all classified as the A_2 subgroup (Fig. 10), which is consistent with their post-collisional characteristics. It is also consistent with the previous studies on the Bayan Obo REE deposit (Ling et al., 2013), i.e., plate subduction during the closure of the Palaeo-Asian Ocean started in the Neoproterozoic (Khain et al., 2003) and lasted until the Carboniferous/Permian (Xiao et al., 2003).

5.2. Relationship to the formation of the Bayan Obo REE deposit

SIMS and LA–ICP-MS zircon dating yields Permian–Triassic $^{206}Pb/^{238}U$ ages ranging from 243.2 to 293.8 Ma (Fig. 12). The Triassic ages (243.2–249.9 Ma) have only been reported by K–Ar and Rb–Sr dating methods (IGCAS, 1988; Zhang et al., 2003), but not by zircon U–Pb dating. The large range of zircon ages reported here indicates a longer period of magmatism than previously identified (Fan et al., 2009; IGCAS, 1988; Ling et al., 2013; Wang et al., 1994; Zhang et al., 2003). The ages are clearly later than the ore forming stage constrained from monazite Th–Pb dating by sensitive high-resolution ion microprobe (SHRIMP) (~750–350 Ma) (Ling et al., 2013) or by solution methods (Chao et al., 1992, 1997; Wang et al., 1994), indicating no contribution to formation of the REE deposit. This is also supported by the initial Nd isotopic ratios of the granitoids, which are distinctively different from those of ore-bearing dolomites (Zhang et al., 2003). However, some of the granitoids show variable LREE enrichment, which may have been gained from the Bayan Obo REE orebodies during granitoid intrusion. All the evidences support that these granitoids have no contribution to the formation of the Bayan Obo deposit. Some of the granitoids have gained the LREE-enriched characteristics from the Bayan Obo deposit, which have minor negative effects on the orebodies.

6. Conclusion

A systematic study on geochronology and geochemistry has been conducted on granitoids of different distances from the Bayan Obo orebodies. The results indicate that these granitoids are peraluminous with A/CNK = 0.99–1.11, LREE enriched and HREE depleted with positive Pb anomaly and negative Nb, Ta, Ti, Eu and Sr anomalies. SIMS and LA–ICP-MS zircon U–Pb dating yield ages between 243.2 and 293.8 Ma. The granitoids plot within the post-collision granite field in the Pearce diagram. Quartz monzonites and one granite have A-type granite characteristics and belong to the A_2 subgroup, indicating a genesis of convergent margins, i.e., plate subduction during the closure of the Palaeo-Asian Ocean started in the Neoproterozoic and ended in the Carboniferous/Permian. The REE patterns and other geochemical characteristics of Bayan Obo granitoids are distinct from those of ore-bearing dolomites, but some of the granitoids show variable LREE enrichments. All the evidences support that these granitoids have made no contribution to the formation of the Bayan Obo deposit. During the Permian–Triassic granitoid intrusion, some of the granitoids have gained the LREE-enriched characteristics from the Bayan Obo orebodies with limited destruction to the orebodies.

Supplementary data to this article can be found online at http://dx.doi.org/10.1016/j.lithos.2014.01.002.

Acknowledgements

The study is financially supported by the National Natural Science Foundation of China (No. 41103006, 41090370 and 41121002), the State Key Laboratory of Isotope Geochemistry (SKLIG-RC-12-02) and the Chinese Academy of Sciences (GIGCAS-135-Y234151001). We thank Ying Liu and Xianglin Tu for help in major and trace element analysis. We highly appreciate Professor Nelson Eby for handling the manuscript and two anonymous reviewers for constructive review comments. This is contribution No. IS-1806 from GIGCAS.

References

Bea, F., Fershtater, G., Corretgé, L.G., 1992. The geochemistry of phosphorus in granite rocks and the effect of aluminium. Lithos 29, 43–56.

Bonin, B., 2007. A-type granites and related rocks: evolution of a concept, problems and prospects. Lithos 97, 1–29.

Chao, E.C.T., Back, J.M., Minkin, J.A., Yinchen, R., 1992. Host-rock controlled epigenetic, hydrothermal metasomatic origin of the Bayan Obo REE–Fe–Nb ore deposit, Inner Mongolia, P.R.C. Applied Geochemistry 7, 443–458.

Chao, E.C.T., Back, J.M., Minkin, J.A., Tatsumoto, M., Wen, W.J., Conrad, J.E., McKee, E.H., Hou, Z.L., Meng, Q.R., Huang, S.G., 1997. U.S. Geological Survey Bulletin 2143: The sedimentary carbonate-hosted giant Bayan Obo REE–Fe–Nb ore deposit of Inner Mongolia, China: A cornerstone example for giant polymetallic ore deposits of hydrothermal origin, Washington.

Drew, L.J., Qingrun, M., Weijun, S., 1990. The Bayan Obo iron rare-earth niobium deposits, Inner-Mongolia, China. Lithos 26, 43–65.

Eby, G.N., 1992. Chemical subdivision of the a-type granitoids — petrogenetic and tectonic implications. Geology 20, 641–644.

Fan, H.R., Hu, F.F., Yang, K.F., Wang, K.Y., Liu, Y.S., 2009. Geochronology framework of late Paleozoic dioritic–granitic plutons in the Bayan Obo area, Inner Mongolia, and tectonic significance. Acta Petrologica Sinica 25, 2933–2938 (in Chinese with English abstract).

Green, T.H., Pearson, N.J., 1986. Ti-rich accessory phase saturation in hydrous mafic–felsic compositions at high P, T. Chemical Geology 54, 185–201.

Harrison, T.M., Watson, E.B., 1984. The behavior of apatite during crustal anatexis — equilibrium and kinetic considerations. Geochimica et Cosmochimica Acta 48, 1467–1477.

Hoskin, P.W.O., Schaltegger, U., 2003. The composition of zircon and igneous and metamorphic petrogenesis. Reviews in Mineralogy and Geochemistry 53, 27–62.

IGCAS, 1988. The Geochemistry of the Bayan Obo Ore Deposit (in Chinese). Science Press, Beijing.

Jahn, B.M., Wu, F.Y., Chen, B., 2000. Massive granitoid generation in Central Asia: Nd isotope evidence and implication for continental growth in the Phanerozoic. Episodes 23, 82–92.

Khain, E.V., Bibikova, E.V., Salnikova, E.B., Kroner, A., Gibsher, A.S., Didenko, A.N., Degtyarev, K.E., Fedotova, A.A., 2003. The Palaeo-Asian ocean in the Neoproterozoic and early Palaeozoic: new geochronologic data and palaeotectonic reconstructions. Precambrian Research 122, 329–358.

Kynicky, J., Smith, M.P., Xu, C., 2012. Diversity of rare earth deposits: the key example of China. Elements 8, 361–367.

Lai, X.D., Yang, X.Y., 2013. Geochemical characteristics of the Bayan Obo giant REE–Nb–Fe deposit: constraints on its genesis. Journal of South American Earth Sciences 41, 99–112.

Lai, X.D., Yang, X.Y., Sun, W.D., 2012. Geochemical constraints on genesis of dolomite marble in the Bayan Obo REE–Nb–Fe deposit, Inner Mongolia: implications for REE mineralization. Journal of Asian Earth Sciences 57, 90–102.

Li, X.H., Liu, Y., Li, Q.L., Guo, C.H., Chamberlain, K.R., 2009. Precise determination of Phanerozoic zircon Pb/Pb age by multicollector SIMS without external standardization. Geochemistry, Geophysics, Geosystems 10. http://dx.doi.org/10.1029/2009GC002400.

Li, C.Y., Zhang, H., Wang, F.Y., Liu, J.Q., Sun, Y.L., Hao, X.L., Li, Y.L., Sun, W.D., 2012. The formation of the Dabaoshan porphyry molybdenum deposit induced by slab rollback. Lithos 150, 101–110.

Li, H., Ling, M.-X., Li, C.-Y., Zhang, H., Ding, X., Yang, X.-Y., Fan, W.-M., Li, Y.-L., Sun, W.-D., 2012. A-type granite belts of two chemical subgroups in central eastern China: indication of ridge subduction. Lithos 150, 26–36.

Liang, J.L., Ding, X., Sun, X.M., Zhang, Z.M., Zhang, H., Sun, W.D., 2009. Nb/Ta fractionation observed in eclogites from the Chinese Continental Scientific Drilling Project. Chemical Geology 268, 27–40.

Ling, M.X., Liu, Y.L., Williams, I.S., Teng, F.Z., Yang, X.Y., Ding, X., Wei, G.J., Xie, L.H., Deng, W.F., Sun, W.D., 2013. Formation of the world's largest REE deposit through protracted fluxing of carbonatite by subduction-derived fluids. Scientific Reports 3. http://dx.doi.org/10.1038/srep01776.

Liu, Y., Liu, H.C., Li, X.H., 1996. Simultaneous and precise determination of 40 trace elements in rock samples using ICP-MS. Geochimica 25, 552–558 (in Chinese with English abstract).

Liu, Y.L., Williams, I.S., Chen, J.F., Wan, Y.S., Sun, W.D., 2008. The significance of paleoproterozoic zircon in carbonatite dikes associated with the Bayan Obo REE–Nb–Fe deposit. American Journal of Science 308, 379–397.

Liu, Y.S., Hu, Z.C., Gao, S., Gunther, D., Xu, J., Gao, C.G., Chen, H.H., 2008. In situ analysis of major and trace elements of anhydrous minerals by LA–ICP–MS without applying an internal standard. Chemical Geology 257, 34–43.

Liu, Y.S., Gao, S., Hu, Z.C., Gao, C.G., Zong, K.Q., Wang, D.B., 2010. Continental and oceanic crust recycling-induced melt–peridotite interactions in the Trans-North China Orogen: U–Pb dating, Hf isotopes and trace elements in zircons from mantle xenoliths. Journal of Petrology 51, 537–571.

Ludwig, K.R., 2012. User's manual for Isoplot 3.75: a geochronological toolkit for Microsoft Excel. Berkeley Geochronology Center Spec. Pub. 5. 75.

Ma, J.L., Wei, G.H., Xu, Y.G., Long, W.G., Sun, W.D., 2007. Mobilization and re-distribution of major and trace elements during extreme weathering of basalt in Hainan Island, South China. Geochimica et Cosmochimica Acta 71, 3223–3237.

Pearce, J.A., 1996. Sources and settings of granitic rocks. Episodes 19, 120–125.

Shand, S.J., 1943. Eruptive Rocks: Their Genesis, Composition, and Classification, with a Chapter on Meteorites. John Wiley & Sons, New York.

Sun, S.S., McDonough, W.F., 1989. Chemical and isotopic systematics of oceanic basalts: implications for mantle composition and processes. In: Saunders, A.D., Norry, M.J. (Eds.), Magmatism in the Ocean Basins. Geological Society of London, London, pp. 313–345.

Sun, W.D., Williams, I.S., Li, S.G., 2002. Carboniferous and Triassic eclogites in the western Dabie Mountains, east-central China: evidence for protracted convergence of the North and South China Blocks. Journal of Metamorphic Geology 20, 873–886.

Tu, G.Z., 1998. The unique nature in ore composition, geological background and metallogenic mechanism of non-conventional superlarge ore deposits: a preliminary discussion. Science in China Series D-Earth Sciences 41, 1–6 (in Chinese with English abstract).

Tu, X.L., Zhang, H., Deng, W.F., Ling, M.X., Liang, H.Y., Liu, Y., Sun, W.D., 2011. Application of RESOlution *in-situ* laser ablation ICP-MS in trace element analyses. Geochimica 40, 83–98 (in Chinese with English abstract).

Wang, K.Y., 1980. Preliminary-study of the distribution pattern of rare-earth elements in granites of Bayan-Obo, Inner Mongolia Autonomous Region. Scientia Geologica Sinica 83–86 (in Chinese with English abstract).

Wang, Z.G., Li, S.B., Su, X.Z., 1973. Geochemistry of sedimentary metamorphism–hydrothermal metasomatism type of REE deposit. Geochimica 1, 5–11 (in Chinese with English abstract).

Wang, J., Tatsumoto, M., Li, X., Premo, W.R., Chao, E.C.T., 1994. A precise ^{232}Th–^{208}Pb chronology of fine-grained monazite: age of the Bayan Obo REE–Fe–Nb ore deposit, China. Geochimica et Cosmochimica Acta 58, 3155–3169.

Watson, E.B., Wark, D.A., Thomas, J.B., 2006. Crystallization thermometers for zircon and rutile. Contributions to Mineralogy and Petrology 151, 413–433.

Xiao, W.J., Windley, B.F., Hao, J., Zhai, M.G., 2003. Accretion leading to collision and the Permian Solonker suture, Inner Mongolia, China: termination of the central Asian orogenic belt. Tectonics 22.

Yang, X.M., Le Bas, M.J., 2004. Chemical compositions of carbonate minerals from Bayan Obo, Inner Mongolia, China: implications for petrogenesis. Lithos 72, 97–116.

Yang, X.M., Yang, X.Y., Fan, H.R., Guo, F., Zhang, Z.F., Zhang, P.S., 2000. Rare earth element geochemistry of the Hercynian granite complex at Baiyunebo, Inner Mongolia, China. Chinese Rare Earths 21, 1–7 (in Chinese with English abstract).

Yang, X.Y., Sun, W.D., Zhang, Y.X., Zheng, Y.F., 2009. Geochemical constraints on the genesis of the Bayan Obo Fe–Nb–REE deposit in Inner Mongolia, China. Geochimica et Cosmochimica Acta 73, 1417–1435.

Yuan, Z.X., Bai, G., Wu, C.Y., Zhang, Z.Q., Ye, X.J., 1992. Geological features and genesis of the Bayan Obo REE ore deposit, Inner-Mongolia, China. Applied Geochemistry 7, 429–442.

Zhang, Z.Q., Yuan, Z.X., Tang, S.H., Bai, G., Wang, J.H., 2003. Age and Geochemistry of the Bayan Obo Ore Deposit. (in Chinese) Geological Publishing House, Beijing.